

Article

Ultra-Deep Oxidative Desulfurization of Fuel with H₂O₂ Catalyzed by Mesoporous Silica-Supported Molybdenum Oxide Modified by Ce

Yang Chen, Qi Tian, Yongsheng Tian *, Jiawei Cui and Guanghui Wang

Hubei Key Laboratory of Coal Conversion and New Carbon Material, School of Chemistry and Chemical Engineering, Wuhan University of Science and Technology, Wuhan 430081, China; ChenYangwust@outlook.com (Y.C.); 15072344500@163.com (Q.T.); cuijiawei_WUST@163.com (J.C.); wangguanghui@wust.edu.cn (G.W.)

* Correspondence: tianyongsheng@wust.edu.cn

Abstract: A mesoporous silica-supported molybdenum oxide catalyst with a cerium(Ce) modifier was prepared by in situ synthesis and used in a hydrogen peroxide (H₂O₂) system for the desulfurization of dibenzothiophene (DBT), benzothiophene (BT), and 4,6-dimethyldibenzothiophene (4,6-DMDBT) fuel oils. The catalytic performance of the catalyst was studied. The catalyst was characterized by Fourier Transform Infra-Red (FT-IR), X-ray diffraction (XRD), Brunner–Emmet–Teller (BET), and X-ray Photoelectron Spectroscopy (XPS). The influences of $m(\text{catalyst})/m(\text{fuel oil})$, $v(\text{H}_2\text{O}_2)/v(\text{fuel oil})$, reaction temperature, and reaction time were investigated. The catalyst had excellent catalytic oxidation desulfurization performance under moderate operational conditions. The catalytic performance was in the order DBT > 4,6-DMDBT > BT. The kinetic analysis results showed that the reaction was a pseudo first-order kinetics process and the apparent activation energies of DBT, BT, and 4,6-DMDBT were 46.67 kJ/mol, 56.23 kJ/mol, and 55.54 kJ/mol, respectively. The reaction products of DBT, BT, and 4,6-DMDBT were DBTO₂, BTO₂, and 4,6-DMDBTO₂, respectively. The recycling experiments indicated that DBT, BT, and 4,6-DMDBT removal could still reach levels of 94.0%, 63.0%, and 77.9% after five cycles.

Keywords: mesoporous silica; molybdenum oxide; cerium; catalytic oxidation desulfurization; kinetics



Citation: Chen, Y.; Tian, Q.; Tian, Y.; Cui, J.; Wang, G. Ultra-Deep Oxidative Desulfurization of Fuel with H₂O₂ Catalyzed by Mesoporous Silica-Supported Molybdenum Oxide Modified by Ce. *Appl. Sci.* **2021**, *11*, 2018. <https://doi.org/10.3390/app11052018>

Academic Editor: Ion Sandu

Received: 31 January 2021

Accepted: 22 February 2021

Published: 25 February 2021

Publisher's Note: MDPI stays neutral with regard to jurisdictional claims in published maps and institutional affiliations.



Copyright: © 2021 by the authors. Licensee MDPI, Basel, Switzerland. This article is an open access article distributed under the terms and conditions of the Creative Commons Attribution (CC BY) license (<https://creativecommons.org/licenses/by/4.0/>).

1. Introduction

Standards related to fuel oils containing sulfur have become more stringent, and various countries are working hard to achieve almost no sulfur in their petrochemical products and fuel oil [1]. Sulfur oxides (SO_x) are produced from sulfur compounds in fuel oil when burned [2] and are one of the main causes of acid rain and air pollution [3]. Catalyst corrosion and deactivation can also be caused by these compounds in the desulfurization procedure [4]. For this reason, the ultra-deep desulfurization of fuel oil is an essential part of the refining industry [5].

Hydrodesulfurization (HDS) is the existing primary traditional and widely used desulfurization process [6]. The hydrodesulfurization catalytic reaction is carried out using hydrogen in the presence of transition metal catalysts [7]. HDS is a common method for removing aliphatic sulfur-containing compounds, but its effect on aromatic sulfur-containing compounds is not good enough [8]. Due to the existence of difficult-to-handle compounds, such as benzothiophene (BT) and its derivative, the existing hydrodesulfurization technology requires more severe operating conditions, which increases operating costs [9]. There are several non-hydrodesulfurization methods such as adsorption desulfurization, alkylation desulfurization, biological desulfurization, extraction desulfurization, oxidative desulfurization, and complex desulfurization [10]. Among them, oxidative desulfurization has received wide application owing to moderate operational conditions and superior

selectivity in removing aromatic sulfur compounds in contrast with HDS, without the need for expensive hydrogen [11]. The oxidative desulfurization process is divided into two stages. First, the sulfur-containing compounds are oxidized to sulfones in the existence of an oxidizer [12]. Second, these sulfones in the mixture are gotten rid of through adsorption.

In catalytic oxidation desulfurization, the oxidant is very important as an indispensable part of the process. The most commonly used oxidants are hydrogen peroxide (H_2O_2), oil-soluble oxidants, gas oxidants, and solid oxidants [13]. Among them, H_2O_2 is currently the most suitable oxidant for oxidative desulfurization [14]. It is cheap and non-corrosive, so it is harmless to the reaction equipment [15]. The catalyst also plays a vital role in the oxidation desulfurization procedure. At present, the most commonly used catalysts are organic acid catalysts, polyoxometalate catalysts, ionic liquids, transition metal oxide catalysts, and inorganic non-metallic catalysts [16]. Among them, molybdenum oxide has received extensive attention. Due to the high valence of Mo and the small ion radius, molybdenum-based catalysts display perfect catalytic performance. Jin [17] et al. reported that Molybdenum trioxide/aluminium oxide (MoO_3/Al_2O_3) was used as a catalyst and H_2O_2 was used as an oxidizer for catalytic oxidative desulfurization, which had good desulfurization performance. At the same time, the catalyst carrier also has a particular influence on the desulfurization performance. Among them, titanium dioxide, activated carbon, alumina, silica, etc., have received extensive attention [18]. Silica is widely used due to its easy production, low price, and rich surface pore structure [19]. Qiu [20] et al. reported the preparation of a mesoporous silica material containing phosphomolybdic acid and investigated its oxidative desulfurization performance. We could ascertain that the removal effect of sulfur compounds was superior. Studies have shown that adding a certain amount of modifier to the catalyst can improve the catalytic performance and selectivity. Transition metal and lanthanides are the most commonly used modifiers. Tian [21] et al. reported that La^{3+} was used as a modifier to prepare a phosphomolybdic acid-supported Silicon dioxide (SiO_2) catalyst. The results illustrated that the catalytic performance was further improved after the modifier was added in comparison to before.

In this work, a $Ce/MoO_3/SiO_2$ catalyst was prepared using an in situ synthesis method with Ce as a modifier. The reaction conditions: $m(\text{catalyst})/m(\text{fuel oil})$, $v(H_2O_2)/v(\text{fuel oil})$, reaction temperature and reaction time, and kinetic analysis of the catalytic reaction and catalyst regeneration were studied. The results showed that the $Ce/MoO_3/SiO_2$ catalyst had excellent desulfurization performance of dibenzothiophene (DBT), BT, and 4,6-dimethyldibenzothiophene (4,6-DMDBT) fuel oil by catalytic oxidation.

2. Materials and Methods

2.1. Materials

Ammonium molybdate tetrahydrate, tetraethyl orthosilicate, hydrogen peroxide (mass fraction 30%), methanol, *n*-octane, and cerium chloride hydrate were produced by Sinopharm Chemical Reagent Co., Ltd.; dibenzothiophene (DBT), benzothiophene (BT), and 4,6-dimethyldibenzothiophene (4,6-DMDBT) were produced by Aladdin; polyethylene oxide-polypropylene oxide-polyethylene oxide triblock copolymer (P123) was produced by Sarn Chemical Technology.

2.2. Catalyst Preparation

For the preparation of the catalyst, 0.44 g $(NH_4)_6Mo_7O_{24} \cdot 4H_2O$ and 0.0596 g $H_{14}CeCl_3O_7$ were first dissolved respectively in 5.0 mL deionized water at room temperature. Next 0.928 g polyethylene oxide-polypropylene oxide-polyethylene oxide triblock copolymer (P123) and 62.0 mL deionized water were added in a 100 mL three-neck flask. After it was completely dissolved, 8.32 g tetraethylorthosilicate was added dropwise at a stirring rate of 600 r/min; stirring continued for 10 min, then $(NH_4)_6Mo_7O_{24} \cdot 4H_2O$ solution was added slowly. After 10 minutes of further reaction, $H_{14}CeCl_3O_7$ solution was added to the reaction system, and the reaction continued for 60 min. After that, the obtained mixture was aged

for 4 h, washed with deionized water, and dried at 105 °C for 12 h. The obtained powder was placed in a tube furnace and roasted at 350 °C for 12 h to obtain the needed catalyst.

2.3. Characterization of the Samples

The FT-IR spectra were recorded on a Bruker VERTEX 70 FT-IR spectrometer, Bruker, Karlsruhe, Germany. The XRD patterns were recorded on a Bruker D8, BrukerAXS, Karlsruhe, Germany. The pore structure of the catalysts was obtained from N₂ adsorption isotherms on an ASAP2460, Micromeritics, Shanghai, China. The XPS measurements were performed with a Thermo Scientific K-Alpha, ThermoFischer, Waltham, MA, America.

2.4. Catalytic Oxidative Desulfurization

The fuel oil with a sulfur content of 400 ppm was obtained by dissolving DBT, BT, and 4,6-DMDBT in *n*-octane in the volumetric flask, respectively. The catalyst was added in a round-bottom flask, 10 mL model fuel oil was added to it, then the flask was placed in a constant temperature water bath under condensing reflux and electromagnetic stirring to heat. When the temperature arrived 40 °C, 50 °C, and 60 °C respectively, 30% H₂O₂ was added to it to carry out a catalytic oxidation desulfurization reaction. After the reaction, the round-bottom flask was quickly taken out and placed in ice water to cool down. After it was sufficiently cooled, the model fuel oil and catalyst were taken out for centrifugal separation. A gas chromatograph was used to detect the sulfur content of the organic phase and calculate the desulfurization rate of the fuel oil.

3. Result and Discussion

3.1. Characterization of Catalysts

Figure 1 shows the FT-IR spectra of ammonium molybdate (a), MoO₃ (b), and Ce/MoO₃/SiO₂ (c). Curve (a) shows an ammonium ion peak at 1404 cm⁻¹, the peaks at 889 cm⁻¹, 839 cm⁻¹, and 642 cm⁻¹ are the molybdate ions peaks. Curve (b) shows that the peaks below 1000 cm⁻¹ are the peaks of the molybdenum oxygen species, and the peak at 988 cm⁻¹ is the peak of the Mo=O. The peaks at 878 cm⁻¹, 821 cm⁻¹, and 673 cm⁻¹ are the peaks of the Mo-O-Mo [22]. Curve (c) shows that the peaks at 805 cm⁻¹ and 1097 cm⁻¹ are the infrared absorption of the carrier silica [23], which caused the molybdenum oxygen species to be covered. It was indicated that in the preparation process of catalyst, ammonium molybdate had been decomposed into MoO₃ and highly dispersed on the catalyst. Catalytic performance for the catalyst was provided by the MoO₃ active center.

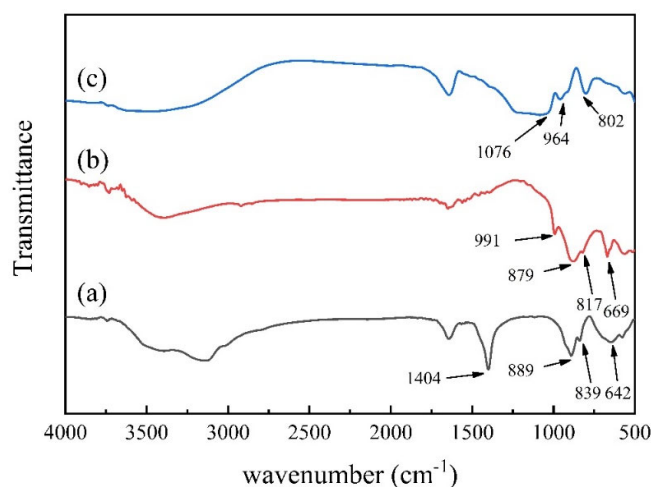


Figure 1. FT-IR spectra of ammonium molybdate (a), MoO₃ (b), and Ce/MoO₃/SiO₂ (c).

Figure 2 shows the powder X-ray diffractions of ammonium molybdate (a), MoO₃ (b), and Ce/MoO₃/SiO₂ (c). Curve (b) shows the diffraction peaks at $2\theta = 12.6^\circ, 18.8^\circ, 22.3^\circ, 25.1^\circ, 26.2^\circ, 27.2^\circ, 29.6^\circ, 30.5^\circ,$ and 38.0° that are attributed to MoO₃ [24]. Curve (c) shows no

obvious characteristic diffraction peak, which illustrated that MoO₃ was evenly dispersed on the catalyst, and that the catalyst Ce/MoO₃/SiO₂ was an amorphous structure.

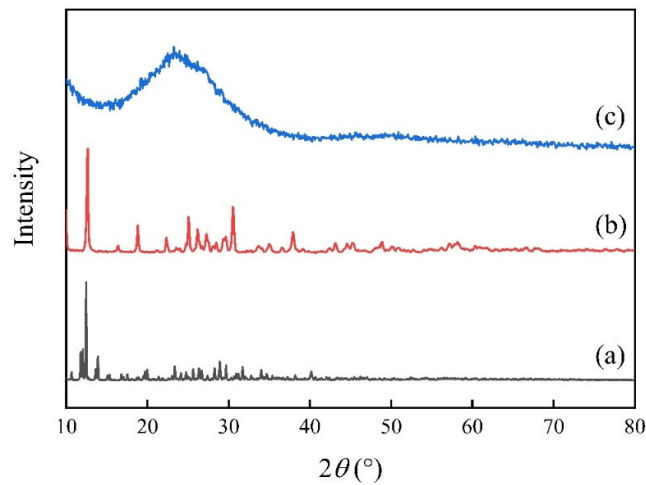


Figure 2. X-ray diffractions of ammonium molybdate (a), MoO₃ (b), and Ce/MoO₃/SiO₂ (c).

Figure 3 shows the N₂ adsorption–desorption isotherm (a) and pore size distribution (b) of Ce/MoO₃/SiO₂. In Figure 3a an obvious hysteresis loop between the relative pressure of 0.60–0.85 is shown. According to the IUPAC classification, this should belong to the type IV adsorption isotherm. This feature was also very consistent with the characteristics of mesoporous materials [25]. In Figure 3b it is shown that the average pore sizes are mainly distributed around 3.35 nm, the specific surface area is 673.133 m²/g, and the pore volume is 0.565 cm³/g. More reaction sites were provided by abundant pore structure and larger specific surface area to accelerate the oxidation reaction rate.

Figure 4 shows the XPS spectra of Ce/MoO₃/SiO₂. In Figure 4a it is shown that the electron binding energy corresponding to Mo 3d in the catalyst is 233.00 eV, indicating the presence of Mo. Since the atomic percentage of Ce was only 0.19%, the characteristic peak of Ce was not detected in the full spectrum. In Figure 4b it is shown that the electron binding energies of Mo 3d_{5/2} and Mo 3d_{3/2} are 233.00 eV and 236.18 eV. According to the comparison of NIST data, it could be concluded that the Mo in the catalyst was +6 formal existence [26]. In Figure 4c it is shown that the electron binding energies corresponding to Ce 3d_{5/2} and Ce 3d_{3/2} are 882.40 eV and 886.39 eV. According to the comparison of NIST data, it could be concluded that the Ce in the catalyst was +4 formal existence [27].

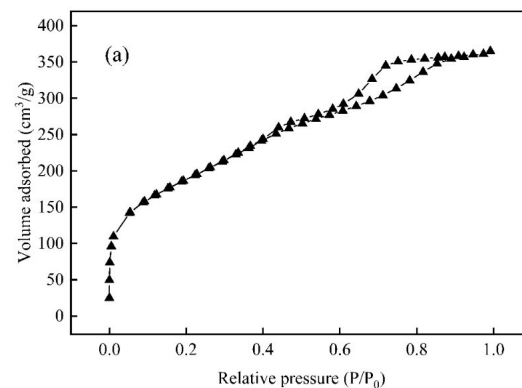


Figure 3. Cont.

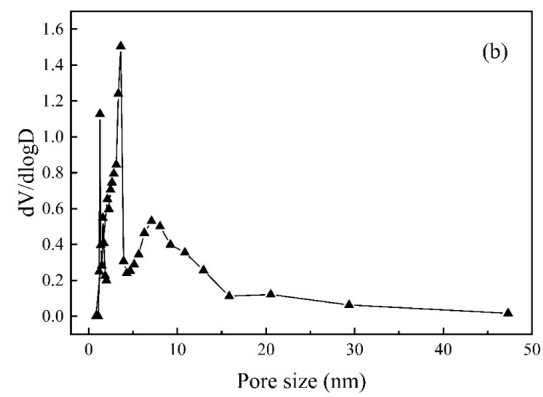


Figure 3. Pore structure parameters of Ce/MoO₃/SiO₂. (a) Adsorption desorption isotherm; (b) pore size distribution.

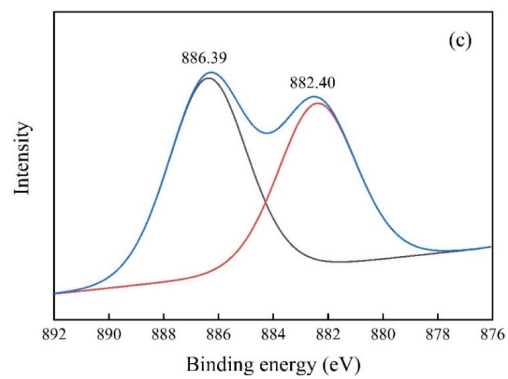
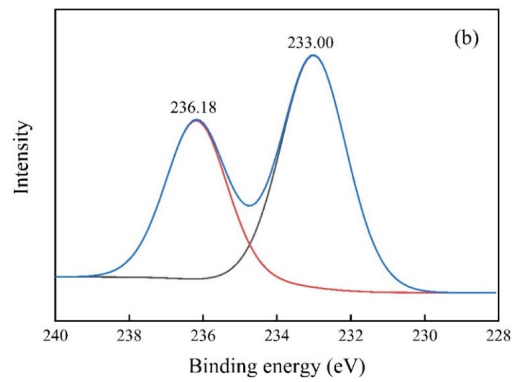
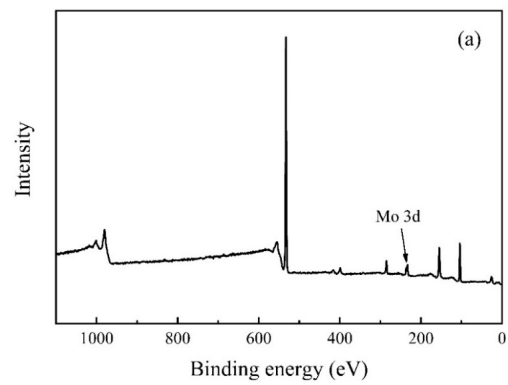


Figure 4. XPS spectra of Ce/MoO₃/SiO₂: (a) survey, (b) Mo 3d, and (c) Ce 3d.

3.2. Oxidative Desulfurization of the Model Oil

To probe the oxidation performance, DBT, BT, and 4,6-DMDBT fuel oil oxidation desulfurization experiments were performed with the catalyst. Figure 5 shows the effect of the $m(\text{catalyst})/m(\text{model oil})$ on the desulfurization rate of 10 mL DBT, BT, and 4,6-DMDBT fuel oil. In Figure 5 it is shown that the desulfurization rate of the DBT, BT, and 4,6-DMDBT fuel oils gradually increased when the $m(\text{catalyst})/m(\text{fuel oil})$ increased, and finally tended to be flat. When the $m(\text{catalyst})/m(\text{fuel oil})$ was 0.018%, the desulfurization rate of DBT and 4,6-DMDBT could be close to 100%, and with BT this rate could be close to 80%.

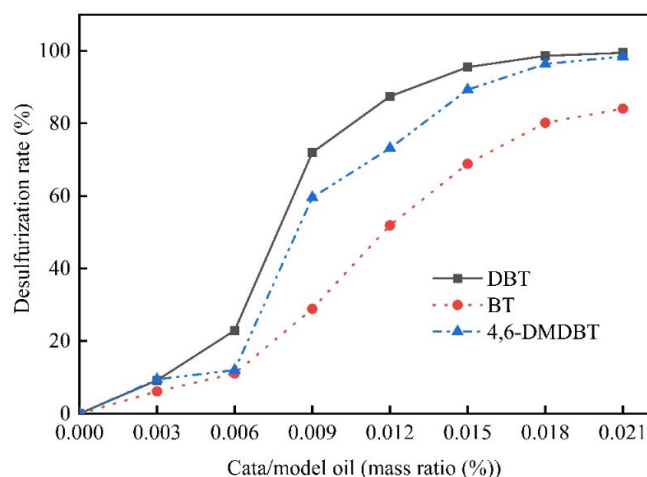


Figure 5. Effect of catalyst/ fuel oil on dibenzothiophene (DBT), benzothiophene (BT), and 4,6-dimethyldibenzothiophene (4,6-DMDBT) desulfurization. Reaction conditions for DBT desulfurization: $v(\text{H}_2\text{O}_2)/v(\text{fuel oil}) = 0.30\%$, $50\text{ }^\circ\text{C}$, 5 min. Reaction conditions for BT desulfurization: $v(\text{H}_2\text{O}_2)/v(\text{fuel oil}) = 0.30\%$, $50\text{ }^\circ\text{C}$, 8 min. Reaction conditions for 4,6-DMDBT desulfurization: $v(\text{H}_2\text{O}_2)/v(\text{fuel oil}) = 0.30\%$, $50\text{ }^\circ\text{C}$, 5 min.

Figure 6 shows the effect of $v(\text{H}_2\text{O}_2)/v(\text{fuel oil})$ on the desulfurization rate of 10 mL DBT, BT, and 4,6-DMDBT fuel oil. In Figure 6 it is shown that the desulfurization rate of the DBT, BT, and 4,6-DMDBT fuel oils first increased then decreased as the $v(\text{H}_2\text{O}_2)/v(\text{model oil})$ increased; when $v(\text{H}_2\text{O}_2)/v(\text{fuel oil})$ was 0.3%, the desulfurization rate of all the DBT, BT, and 4,6-DMDBT fuel oils reached the maximum. Within a certain range, the amount of peroxopolymetallic compound increased with the amount of the oxidant H_2O_2 , which formed by combining with the active center of ammonium molybdate, thereby speeding up the reaction rate. When the amount exceeded the optimal amount, the water generated by the H_2O_2 reaction led to the production of a two-phase system, which may have reduced the catalyst's dispersion in the oil phase, causing a decrease in the reaction rate [28].

Figure 7 shows the effect of reaction temperature and reaction time on the desulfurization rate of DBT, BT, and 4,6-DMDBT. At the same reaction temperature, the desulfurization rate of DBT, BT, and 4,6-DMDBT fuel oils gradually increased while the reaction time increased. Simultaneously, the desulfurization rate of DBT, BT, and 4,6-DMDBT fuel oils steadily increased with the increase of reaction temperature. When the reaction temperature increased, the thermal motion between molecules was increased [29]. At the same time, the number of metal peroxides generated by MoO_3 and H_2O_2 in the fuel oil was increased while the reaction time increased, which provided more catalytic activity sites, thereby accelerating the reaction rate [30]. At $60\text{ }^\circ\text{C}$, the desulfurization rate of DBT was close to 100% at 5 min, the desulfurization rate of 4,6-DMDBT was close to 100% at 6 min, and the desulfurization rate of BT was close to 100% at 12 min. Under the same reaction conditions, the oxidation performance of the sulfur compounds decreased in the order of $\text{DBT} > 4,6\text{-DMDBT} > \text{BT}$. Due to the electron cloud density of sulfur atoms on BT being smaller than on DBT and 4,6-DMDBT, BT was more challenging to remove than DBT and 4,6-DMDBT [31]. Although the electron cloud density of 4,6-DMDBT was bigger than DBT,

4,6-DMDBT had two methyl groups, which increased steric hindrance. Thus, 4,6-DMDBT was more difficult to remove than DBT.

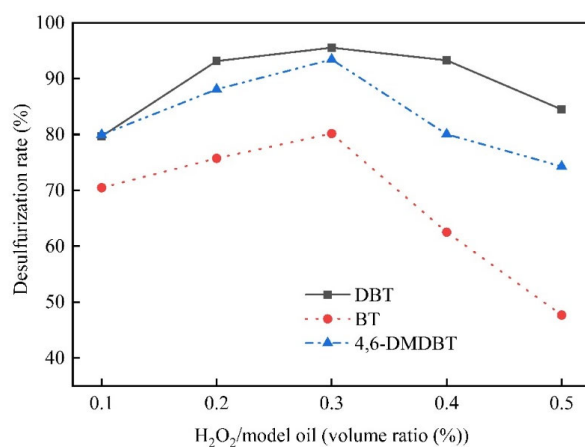


Figure 6. Effect of H₂O₂/fuel oil on DBT, BT, and 4,6-DMDBT desulfurization. Reaction conditions for DBT desulfurization: $m(\text{catalyst})/m(\text{fuel oil}) = 0.018\%$, 50 °C, 5 min. Reaction conditions for BT desulfurization: $m(\text{catalyst})/m(\text{fuel oil}) = 0.018\%$, 50 °C, 8 min. Reaction conditions for 4,6-DMDBT desulfurization: $m(\text{catalyst})/m(\text{fuel oil}) = 0.018\%$, 50 °C, 5 min.

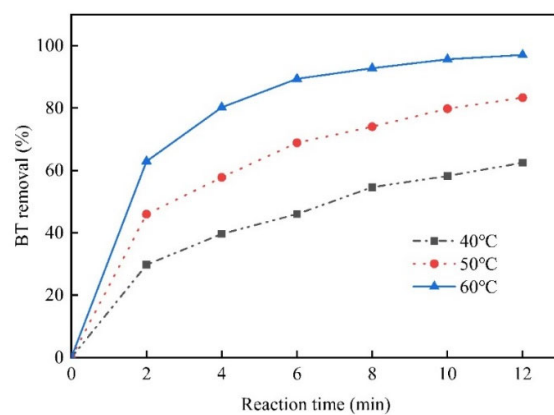
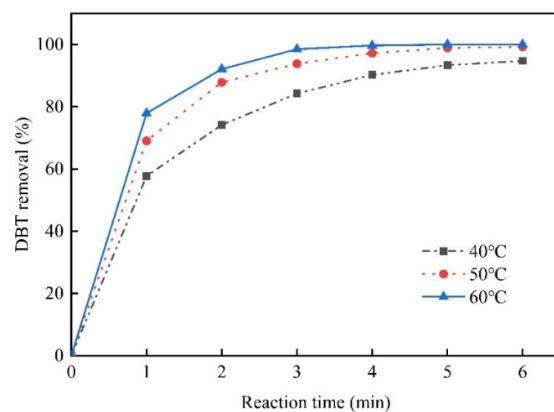


Figure 7. Cont.

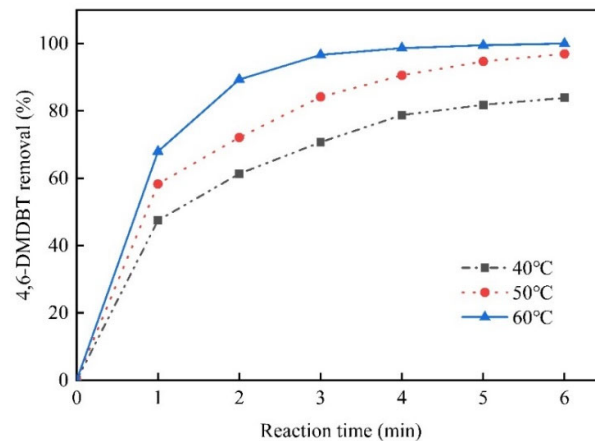


Figure 7. Effect of reaction time on DBT, BT, and 4,6-DMDBT desulfurization. Reaction conditions for DBT desulfurization: $m(\text{catalyst})/m(\text{fuel oil}) = 0.018\%$, $v(\text{H}_2\text{O}_2)/v(\text{fuel oil}) = 0.30\%$, $T = 40^\circ\text{C}$, 50°C , and 60°C . Reaction conditions for BT desulfurization: $m(\text{catalyst})/m(\text{fuel oil}) = 0.018\%$, $v(\text{H}_2\text{O}_2)/v(\text{fuel oil}) = 0.30\%$, $T = 40^\circ\text{C}$, 50°C , and 60°C . Reaction conditions for 4,6-DMDBT desulfurization: $m(\text{catalyst})/m(\text{fuel oil}) = 0.018\%$, $v(\text{H}_2\text{O}_2)/v(\text{fuel oil}) = 0.30\%$, $T = 40^\circ\text{C}$, 50°C , and 60°C .

3.3. Apparent Activation Energy and Reaction Rate Constant

Table 1 lists the reaction rate constants and correlation coefficients of DBT, BT, and 4,6-DMDBT at different temperatures. By fitting the relationship between the desulfurization rate and the reaction time of DBT, BT, and 4,6-DMDBT fuel oils at different temperatures, the least squares method was used to obtain the relationship between the reaction time t and $\ln(1/(1-x_T))$. Figure 8 uses the Arrhenius formula to calculate the apparent activation energy. In Figure 8 it is shown that the catalytic oxidation reaction satisfied the pseudo first-order kinetics, and the apparent activation energies of DBT, BT, and 4,6-DMDBT were 46.67 kJ/mol, 56.23 kJ/mol, and 55.54 kJ/mol, respectively. The apparent activation energy was in the order $\text{BT} > 4,6\text{-DMDBT} > \text{DBT}$.

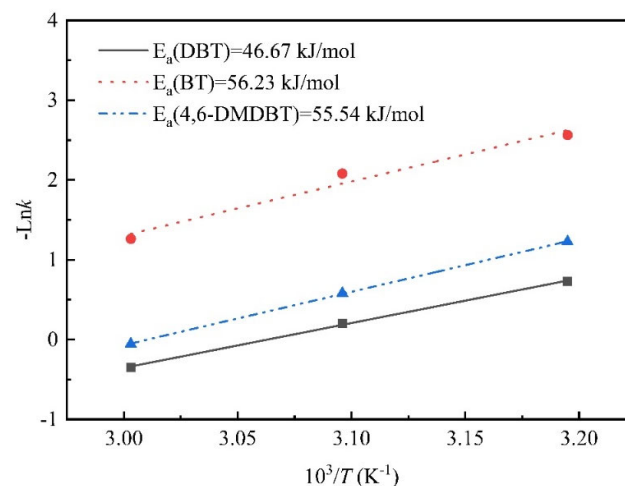


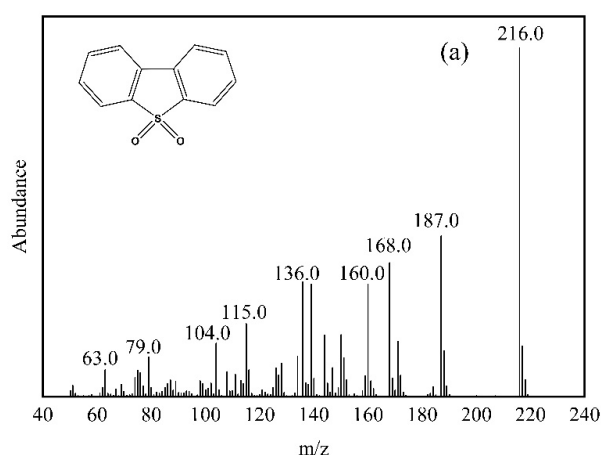
Figure 8. Arrhenius activation energies for DBT, BT, and 4,6-DMDBT oxidation.

Table 1. The reaction rate constant (k) and correlation coefficient (R^2) for the oxidation reactions of DBT, BT, and 4,6-DMDBT at different temperatures.

Sample	$t(^{\circ}\text{C})$	$k(\text{min}^{-1})$	R^2
DBT	40	0.482	0.973
DBT	50	0.815	0.987
DBT	60	1.416	0.995
BT	40	0.077	0.955
BT	50	0.140	0.960
BT	60	0.283	0.974
4,6-DMDBT	40	0.293	0.943
4,6-DMDBT	50	0.559	0.994
4,6-DMDBT	60	1.056	0.998

3.4. Analysis of Oxidation Product

To research the reaction product of catalytic oxidation, Gas chromatography-mass spectrometry (GC-MS) was used to detect the composition of the reaction product. The catalyst and the model fuel oil were centrifuged after the catalytic oxidation desulfurization reaction. The components in the oil phase were detected, and the catalyst was washed with methanol and centrifuged to detect the components in the methanol phase. Figure 9 shows the MS spectra of DBT, BT, and 4,6-DMDBT in the methanol phase. The peaks at m/z 216, 166, and 244 are dibenzothiophene sulfone (DBTO₂), benzothiophene sulfone (BTO₂), and 4,6-dimethyldibenzothiophene sulfone (4,6-DMDBTO₂). Compared with standard data, the reaction products of DBT, BT, and 4,6-DMDBT were DBTO₂, BTO₂ and 4,6-DMDBTO₂. Since no sulfur compounds and their respective oxidation products were detected in the oil phase, it indicated that DBTO₂, BTO₂, and 4,6-DMDBTO₂ were highly polar and readily adsorbed by the solid catalyst, which solved the problem of separation of oxidation products and oil phase. The Mo⁶⁺ on the catalyst first reacted with hydrogen peroxide to form a molybdenum-based peroxide. The molybdenum-based peroxide reacted with sulfur atoms in the sulfur-containing compounds to form sulfoxide and water. The active sites of Mo⁶⁺ were released, and then reacted with hydrogen peroxide to form a molybdenum-based peroxide. The molybdenum-based peroxide reacted with the sulfur atoms in the sulfoxide to form sulfone and water. The active sites of Mo⁶⁺ were released again. After the reaction, the sulfone was adsorbed by the catalyst. After washing with methanol, the sulfone substances adsorbed on the catalyst were removed, and the catalyst could be recycled.

**Figure 9.** Cont.

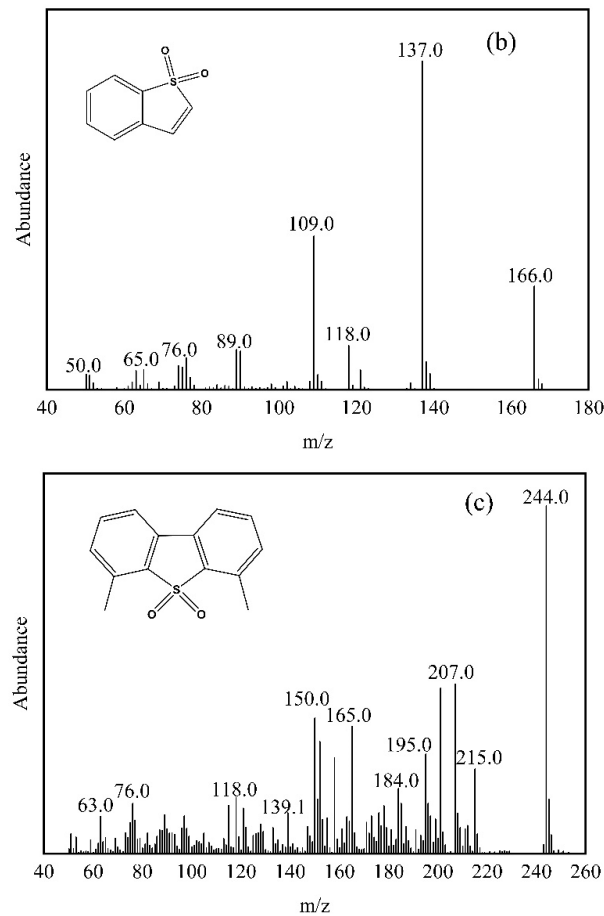


Figure 9. (a–c) MS spectra of the oxidized products of DBT, BT, and 4,6-DMDBT.

3.5. Reuse Cycles of the Catalysts

To research the reusable performance of the catalyst, the reacted catalyst and the model fuel oil were centrifuged to detect the content of sulfur compounds and calculate the desulfurization rate. The solid catalyst was recovered, washed with methanol, and placed in a 105 °C drying oven to dry and regenerate. The catalyst was used again under the same reaction conditions, for a new round of catalytic oxidation desulfurization reactions. Figure 10 shows the reusable performance of the catalyst. The desulfurization rates of the DBT, BT, and 4,6-DMDBT fuel oils dropped to 94.0%, 63.0%, and 77.9% after five times of repeated use.

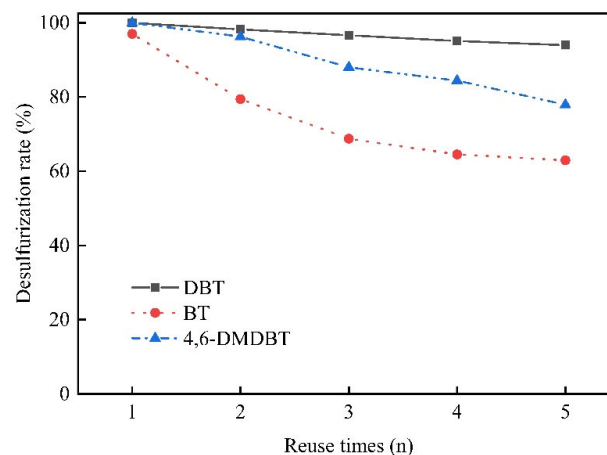


Figure 10. Effect of reuse times on the oxidative desulfurization rate of DBT, BT, and 4,6-DMDBT.

4. Conclusions

In this work, a Ce/MoO₃/SiO₂ catalyst was prepared by an in situ synthesis method with Ce as a modifier. In the H₂O₂ system, DBT, BT, and 4,6-DMDBT could be oxidized and desulfurized under mild reaction conditions, showing excellent catalytic activity. The kinetic analysis results showed that the reaction was pseudo first-order kinetics. The apparent activation energies of DBT, BT, and 4,6-DMDBT were 46.67 kJ/mol, 56.23 kJ/mol, and 55.54 kJ/mol. The catalytic oxidation reaction products were DBTO₂, BTO₂, and 4,6-DMDBTO₂, which were easily adsorbed and separated from the reaction mixture by the solid catalyst due to their strong polarity. The desulfurization rates of the catalyst after five times repeated use for the DBT, BT, and 4,6-DMDBT fuel oils were 94.0%, 63.0%, and 77.9%.

Author Contributions: Methodology, Y.C. and Q.T.; software, Q.T. and J.C.; data curation, Q.T.; writing—original draft preparation, Y.C.; writing—review and editing, G.W. and Y.T.; project administration, G.W.; funding acquisition, G.W. and Y.T. All authors have read and agreed to the published version of the manuscript.

Funding: This research was funded by Supported by National Key R&D Program of China (No. 2017YFB0304300&2017YFB0304303) and the National Natural Science Foundation (No. 21473126).

Institutional Review Board Statement: Not applicable.

Informed Consent Statement: Not applicable.

Data Availability Statement: Data available in a publicly accessible repository.

Conflicts of Interest: The authors declare no conflict of interest.

References

1. Hossain, M.N.; Park, H.C.; Choi, H.S. A Comprehensive Review on Catalytic Oxidative Desulfurization of Liquid Fuel Oil. *Catalysts* **2019**, *9*, 229. [[CrossRef](#)]
2. Yang, C.; Zhao, K.; Cheng, Y.; Zeng, G.; Zhang, M.; Shao, J.; Lu, L. Catalytic oxidative desulfurization of BT and DBT from n-octane using cyclohexanone peroxide and catalyst of molybdenum supported on 4A molecular sieve. *Sep. Purif. Technol.* **2016**, *163*, 153–161. [[CrossRef](#)]
3. Tao, X.; Zhou, Y.; Wei, Q.; Ding, S.; Zhou, W.; Liu, T.; Li, X. Inhibiting effects of nitrogen compounds on deep hydrodesulfurization of straight-run gas oil over a NiW/Al₂O₃ catalyst. *Fuel* **2017**, *188*, 401–407. [[CrossRef](#)]
4. De Luna, M.D.G.; Futralan, C.M.; Duavis, A.G.; Wan, M.-W. Optimization and kinetics of the desulfurization of diesel fuel via high shear mixing oxidation assisted by adsorption of sulfones onto chitosan-coated bentonite. *Int. J. Green Energy* **2018**, *15*, 930–940. [[CrossRef](#)]
5. Zhang, B.; Jiang, Z.; Li, J.; Zhang, Y.; Lin, F.; Liu, Y.; Li, C. Catalytic oxidation of thiophene and its derivatives via dual activation for ultra-deep desulfurization of fuels. *J. Catal.* **2012**, *287*, 5–12. [[CrossRef](#)]
6. Lai, W.; Chen, Z.; Zhu, J.; Yang, L.; Zheng, J.; Yi, X.; Fang, W. A NiMoS flower-like structure with self-assembled nanosheets as high-performance hydrodesulfurization catalysts. *Nanoscale* **2016**, *8*, 3823–3833. [[CrossRef](#)]
7. Hajjar, Z.; Kazemeini, M.; Rashidi, A.; Bazmi, M. Graphene based catalysts for deep hydrodesulfurization of naphtha and diesel fuels: A physiochemical study. *Fuel* **2016**, *165*, 468–476. [[CrossRef](#)]
8. Tavizón-Pozos, J.A.; Suárez-Toriello, V.A.; Reyes, J.A.D.L.; Guevara-Lara, A.; Pawelec, B.; Fierro, J.L.G.; Vrinat, M.; Geantet, C. Deep Hydrodesulfurization of Dibenzothiophenes over NiW Sulfide Catalysts Supported on Sol–Gel Titania–Alumina. *Top. Catal.* **2015**, *59*, 241–251. [[CrossRef](#)]
9. Song, S.; Yang, X.; Wang, B.; Zhou, X.; Duan, A.; Chi, K.; Zhao, Z.; Xu, C.; Chen, Z.; Li, J. Al-modified mesocellular silica foam as a superior catalyst support for dibenzothiophene hydrodesulfurization. *Chin. J. Catal.* **2017**, *38*, 1347–1359. [[CrossRef](#)]
10. Zhou, W.; Liu, M.; Zhou, Y.; Wei, Q.; Zhang, Q.; Ding, S.; Zhang, Y.; Yu, T.; You, Q. 4,6-Dimethyldibenzothiophene Hydrodesulfurization on Nickel-Modified USY-Supported NiMoS Catalysts: Effects of Modification Method. *Energy Fuels* **2017**, *31*, 7445–7455. [[CrossRef](#)]
11. Abdi, G.; Ashokkumar, M.; Alizadeh, A. Ultrasound-assisted oxidative-adsorptive desulfurization using highly acidic graphene oxide as a catalyst-adsorbent. *Fuel* **2017**, *210*, 639–645. [[CrossRef](#)]
12. Bonde, S.E.; Gore, W.; Dolbear, G.E.; Skov, E.R. Selective oxidation and extraction of sulfur-containing compounds to economically achieve ultra-low proposed diesel fuel sulfur requirements. *Prepr. Am. Chem. Soc. Div. Pet. Chem.* **2000**, *45*, 364–366. [[CrossRef](#)]
13. Zheng, M.; Xu, C.; Hu, H.; Ye, Z.; Chen, X. A modified homogeneous surface diffusion model for the fixed-bed adsorption of 4,6-DMDBT on Ag–CeO_x/TiO₂–SiO₂. *RSC Adv.* **2016**, *6*, 112899–112907. [[CrossRef](#)]
14. Sudhir, N.; Yadav, P.; Nautiyal, B.; Singh, R.; Rastogi, H.; Chauhan, H. Extractive desulfurization of fuel with methyltriphenyl phosphonium bromide- tetraethylene glycol-based eutectic solvents. *Sep. Sci. Technol.* **2020**, *55*, 554–563. [[CrossRef](#)]

15. Kang, Y.; Shao, D.; Li, N.; Yang, G.; Zhang, Q.; Zeng, L.; Luo, J.; Zhong, W. Cancer risk assessment of human exposure to polycyclic aromatic hydrocarbons (PAHs) via indoor and outdoor dust based on probit model. *Environ. Sci. Pollut. Res.* **2014**, *22*, 3451–3456. [[CrossRef](#)]
16. Dou, S.-Y.; Wang, R. Recent Advances in New Catalysts for Fuel Oil Desulfurization. *Curr. Org. Chem.* **2017**, *21*, 1019–1036. [[CrossRef](#)]
17. Jin, W.; Tian, Y.; Wang, G.; Zeng, D.; Xu, Q.; Cui, J. Ultra-deep oxidative desulfurization of fuel with H₂O₂ catalyzed by molybdenum oxide supported on alumina modified by Ca²⁺. *RSC Adv.* **2017**, *7*, 48208–48213. [[CrossRef](#)]
18. Chang, J.; Wang, A.; Liu, J.; Li, X.; Hu, Y. Oxidation of dibenzothiophene with cumene hydroperoxide on MoO₃/SiO₂ modified with alkaline earth metals. *Catal. Today* **2010**, *149*, 122–126. [[CrossRef](#)]
19. Zhang, M.; Zhu, W.; Li, H.; Xun, S.; Li, M.; Li, Y.; Wei, Y.; Li, H. Fabrication and characterization of tungsten-containing mesoporous silica for heterogeneous oxidative desulfurization. *Chin. J. Catal.* **2016**, *37*, 971–978. [[CrossRef](#)]
20. Qiu, J.; Wang, G.; Zhang, Y.; Zeng, D.; Chen, Y. Direct synthesis of mesoporous H₃PMo₁₂O₄₀/SiO₂ and its catalytic performance in oxidative desulfurization of fuel oil. *Fuel* **2015**, *147*, 195–202. [[CrossRef](#)]
21. Tian, Y.; Wang, G.; Long, J.; Cui, J.; Jin, W.; Zeng, D. Ultra-deep oxidative desulfurization of fuel with H₂O₂ catalyzed by phosphomolybdic acid supported on silica. *Chin. J. Catal.* **2016**, *37*, 2098–2105. [[CrossRef](#)]
22. Seguin, L.; Figlarz, M.; Cavagnat, R.; Lassègues, J.-C. Infrared and Raman spectra of MoO₃ molybdenum trioxides and MoO₃·xH₂O molybdenum trioxide hydrates. *Spectrochim. Acta Part A: Mol. Biomol. Spectrosc.* **1995**, *51*, 1323–1344. [[CrossRef](#)]
23. Ravikumar, R.; Sundeeep, D.; Krishna, A.G.; Ephraim, S.D.; Ali, A.; Ahmed, S.I.; Manikanta, K.; Kumar, T.V. Spectral Investigation of Structural and Optical Properties of Mechanically Synthesized TiO₂-V₂O₅ Nanocomposite Powders. *Mater. Today: Proc.* **2016**, *3*, 31–38. [[CrossRef](#)]
24. Du, K.; Wei, R.H.; Bai, Y.N.; Gu, Y.; Ben Li, L. Synthesis of MoO₃ Nanostructures by a Solution Method. *Adv. Mater. Res.* **2012**, *554*, 494–497. [[CrossRef](#)]
25. Sing, K.S.W. Reporting physisorption data for gas/solid systems with special reference to the determination of surface area and porosity (Recommendations 1984). *Pure Appl. Chem.* **1985**, *57*, 603–619. [[CrossRef](#)]
26. Chary, K.V.R. Structure and catalytic properties of molybdenum oxide catalysts supported on zirconia. *J. Catal.* **2004**, *226*, 283–291. [[CrossRef](#)]
27. Eighmy, T.T. Hinsdalite (PbAl₃PO₄SO₄(OH)₆) Characterized by XPS: An Environmentally Important Secondary Mineral. *Surf. Sci. Spectra* **1999**, *6*, 184–192. [[CrossRef](#)]
28. Long, Z.; Yang, C.; Zeng, G.; Peng, L.; Dai, C.; He, H. Catalytic oxidative desulfurization of dibenzothiophene using catalyst of tungsten supported on resin D152. *Fuel* **2014**, *130*, 19–24. [[CrossRef](#)]
29. Guo, Z.; Du, Y.; Lei, J.; Zhou, L.; Du, X. Oxidative Desulfurization of Fuel Oil at Room Temperature Catalyzed by Ordered Meso-macroporous HPW/SiO₂. *J. Wuhan Univ. Technol. Sci. Ed.* **2019**, *34*, 1071–1076. [[CrossRef](#)]
30. Li, L.; Lu, Y.; Meng, H.; Li, C. Lipophilicity of amphiphilic phosphotungstates matters in catalytic oxidative desulfurization of oil by H₂O₂. *Fuel* **2019**, *253*, 802–810. [[CrossRef](#)]
31. Jatav, S.; Srivastava, V.C. Ce/Al₂O₃ as an efficient catalyst for oxidative desulfurization of liquid fuel. *Pet. Sci. Technol.* **2019**, *37*, 633–640. [[CrossRef](#)]